ACS APPLIED MATERIALS & INTERFACES

Research Article

Cite This: ACS Appl. Mater. Interfaces 2018, 10, 23638−23646

www.acsami.org

Increasing the Resistance of Living Cells against Oxidative Stress by Nonnatural Surfactants as Membrane Guards

Marius Kunkel, Stefan Schildknecht, Klaus Boldt, Lukas Zeyffert, David Schleheck, Marcel Leist, and Sebastian Polarz*

University of Konstanz, Universitätsstrasse 10, 78457 Konstanz, Germany

Supporting Information

ABSTRACT: The importation of construction principles or even constituents from biology into materials science is a prevailing concept. Vice versa, the cellular level modification of living systems with nonnatural components is much more difficult to achieve. It has been done for analytical purposes, for example, imaging, to learn something about intracellular processes. Cases describing the improvement of a biological function by the integration of a nonnatural (nano)constituent are extremely rare. Because biological membranes contain some kind of a surfactant, for example, phospholipids, our idea is to modify cells with a newly synthesized surfactant. However, this surfactant is intended to possess an additional functionality, which is the reduction of oxidative stress. We report the synthesis of a surfactant with Janus-type head group architecture, a fullerene C_{60} modified by five alkyl chains on one side and an average of 20 oxygen species on the other hemisphere. It is demonstrated that the amphiphilic properties of the fullerenol surfactant are similar to that of lipids. Not only quenching of reactive oxygen species (superoxide, hydroxyl radicals, peroxynitrite, and hydrogen peroxide) was successful, but also the fullerenol surfactant exceeds benchmark antioxidant agents such as quercetin. The surfactant was then brought into contact with different cell types, and the viability even of delicate cells such as human liver cells (HepG2) and human dopaminergic neurons (LUHMES) has proven to be extraordinarily high. We could show further that the cells take up the fullerenol surfactant, and as a consequence, they are protected much better against oxidative stress.

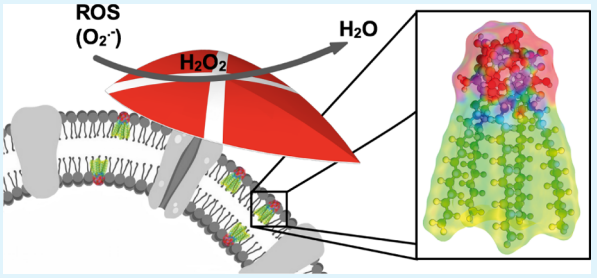

KEYWORDS: *surfactant, amphiphile, fullerenol, fullerene, ROS quenching, superoxide, membrane, living cells*

INTRODUCTION

Because of the exponentially growing global population, we will have to provide more commodities than have ever been produced before. In addition to the extension and improvement of the capacities of chemical industry as we know, a seminal approach is to use microbes in chemical factories.[1,2] One of the problems involved in realizing this goal is that many cells, prokaryotes as well as eukaryotes, are sensitive to oxidative stress.[3] Reactive oxygen species (ROS) are in any case major reasons for cellular damages and aging processes. Anaerobic microorganisms are of course even more sensitive to an oxygen-rich environment. In particular, in an aqueous dispersion and in contact to daylight, there is an inevitable level of ROS such as the superoxide anion, hydroxyl radicals, or singlet oxygen. Evolution has countered this problem by the development of cellular mechanisms for self-protection against those species by scavenging enzymes such as superoxide dismutase.[4] However, if the oxidative stress level becomes too high or occurs very fast, the biological protection alone is not sufficient anymore, which then results in damages and diseases associated with oxidative stress.[5] Therefore, it would be highly interesting to aid cells and to increase their resistance against ROS.

Fullerene derivatives have been evaluated for biomedical use for quite some time. Depending on their modification, they have shown promising results as antiviral, antibacterial, or antioxidative compounds. However, a huge disadvantage of most fullerene derivatives is their poor solubility in water, which is of course pivotal for most biomedical usage. One approach for making them more suitable for applications in biotechnology is the formation of hybrids with phospholipids, the so-called fullerene liposomes. The encapsulation of fullerene derivatives in liposomes or the direct interaction with cell membranes can lower the compound's toxicity and enhance its bioavailability. Another approach is the use of water-soluble derivatives such as polyhydroxylated fullerenes, the so-called fullerenols.[6,7] It has been reported that these compounds can reliably quench ROS in aqueous systems.[8−11] Fullerenols can even penetrate the cellular membranes and accumulate inside the cell, where they possibly aggregate. Unfortunately, it was found that the presence of fullerenols in the internal regions of the cell is harmful and can even lead to necrosis. Besides ill-defined accumulation, there are also other

Received: April 30, 2018
Accepted: June 27, 2018
Published: June 27, 2018

DOI: 10.1021/acsami.8b07032
ACS Appl. Mater. Interfaces 2018, 10, 23638−23646

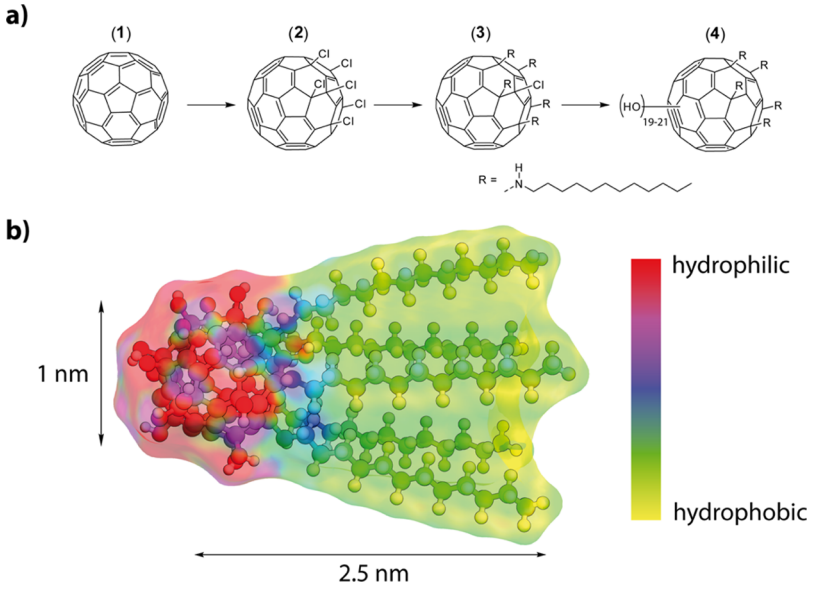

Figure 1. (a) Synthesis sequence to derive surfactants with a fullerenol head group. (b) Optimized molecular structure of surfactant (**4**) with dimensions and electrostatic potential map.

reasons for the toxicity of fullerene derivatives in cellular systems. The solubility of the compound, functional groups, and the degree of derivatization influence the compound's toxicity.[11,12]

Because of the argument given above, one has to effectively suppress the undesired aggregation of fullerenols. Further, they would ideally remain as guards against oxidative stress integrated in the cellular membrane instead of entering the cell. The importance of the exact positioning of the fullerenol entities was also discussed by Nakamura et al. in a theoretical study in 2017.[13] Because cellular membranes mainly consist of phospholipids, our idea is to generate a new surfactant showing lipid-like behavior and a fullerenol head group as the entity capable of protection against oxidative stress via catalytic conversion of ROS into less harmful compounds. A great body of work exists on amphiphiles containing fullerenes.[14,15] Amphiphilic fullerenes are known for forming bi- or multilayered vesicular aggregates in solution.[16−19] They have also been explored for biochemical applications.[14,20,21] The work of Hirsch et al. needs to be mentioned in this context, who synthesized membrane-forming hexa-adducts of C_{60}.[22] These compounds can, for example, be used as nanocarriers for drug delivery systems.[21,23] The vesicular self-assembly of amphiphilic fullerenes was also investigated by Nakamura et al. They showed that different kinds of fullerene amphiphiles aggregate in a membrane-like structure.[16,19,24] However, the fullerene is part of the hydrophobic moiety in most cases. True surfactants, in which the fullerene represents the hydrophilic head group, are rare.[25−28]

In this paper, we report the synthesis and characterization of a surfactant (see Figure 1) comprising a fullerenol head group. After characterization of its surfactant and self-assembly properties, we will test the ROS deactivation features. Finally, the biocompatibility of the surfactant will be explored, and the protection of cells against oxidative stress will be tested.

RESULTS AND DISCUSSION

Surfactant Preparation. We achieved the synthesis of the Janus-type target molecule (**4**) as follows (Figure 1a,b). The method published by Kuvychko et al. was applied to obtain hexa-chlorination selectively on only one side of C_{60} (**2**).[29] Penta-alkylation with dodecyl amine was achieved by adapting a protocol published by Kornev et al.[30] to obtain the precursor molecule (**3**). ^{1}H NMR, ^{13}C NMR, and matrix-assisted laser desorption ionization mass spectrometry (MALDI-MS) could confirm the penta-alkylation. This can clearly be seen in the ^{1}H NMR. Besides the signals for the alkyl chains, it shows the signals of the secondary amines bound to the fullerene core as five triplets centered at 3.22 ppm (see the Supporting Information, Figure S1). Also, the ^{13}C NMR shows distinct signals for the sp^{3}-hybridized carbons of the fullerene core at which the chains are attached at 66, 68.2, and 69.4 ppm. Three signals can be observed because of the 2:2:1 symmetry (see the Supporting Information, Figure S2). The MALDI-MS reveals the M − HCl peak at m/z = 1641.6 (1641.3). In the last step, the hydroxyl moieties are introduced to the precursor using NaOH and H_2O_2 (see also the experimental part). The fullerenol surfactant (**4**) was characterized by a combination of methods. Fourier transform infrared (FT-IR) spectroscopy confirms the polyhydroxylation of precursor (**3**). The observed spectrum is in agreement with the characteristics compared to fullerenols found in the literature.[31−33] Signals at 3365, 1410, and 1032 cm^{-1} can be assigned to the hydroxyl moieties. Weak signals at 2971 and 2942 cm^{-1} fit to the attached alkyl chains. Furthermore, a strong signal at 1645 cm^{-1} indicates the presence of hemiketal moieties which include the hydroxyl groups (shown in the Supporting Information, Figure S3).[34,35] The ^{13}C NMR spectrum (see the Supporting Information, Figure S4) is also in full agreement with the proposed structure and confirms that the scaffold of the precursor is still intact. The alkyl chains are located between 13 and 40 ppm. Signals at 52.4, 57.2, and 57.3 ppm fit the carbons of the fullerene at which the alkyl amines are attached to. Three signals are observed because they have a 2:2:1 symmetry. Because the hydroxyl groups are not introduced by substitution of, for example, halogens but directly to the fullerene core, one needs to determine the degree of poly-hydroxylation and the kind of the attached oxygen species. Therefore, thermogravimetric

DOI: 10.1021/acsami.8b07032
ACS Appl. Mater. Interfaces 2018, 10, 23638−23646

analysis (TGA) was performed among others (shown in the Supporting Information, Figure S5). We assign the mass loss below 200 °C to the removal of water loosely bound to the head group via hydrogen bonding. The mass loss at a higher temperature (Δm = −17.05%) fits to the elimination of hydroxyl groups and vinyl ethers (hemiketals).[36] The latter mass loss corresponds to an average number of ≈20 ± 1 oxygen species attached to C_{60} in (**4**). The penta-alkylated fullerene remains after the loss of the oxygen species. The successful synthesis and structure of the surfactant could be confirmed conclusively by MALDI-MS (shown in the Supporting Information, Figure S6). All signals of the complex fragmentation pattern could also be assigned by comparison with fullerenol compounds known in the literature.[37,38] Every signal belongs to a singly charged species and can be assigned with the following formula: $[M - (v - 1)H - w(OH) - xH_2O - yNH - zC_{12}H_{25}]^+$. Like for other fullerenols, the hydroxyl groups are released as water, generating an oxygen radical species or hydroxyl radicals. Furthermore, the chains can be released with or without the amine linker. A maximum of five chains can be detected, which fits the findings from the NMR. As a result of these decomposition mechanisms, no molecular ion peak can be observed. Though MALDI-MS reveals a mixture of different oxygen species, a maximum number of 21 oxygen species could be detected, which is in agreement with the results from the TGA. Further information about the degree of poly-hydroxylation and the kind of oxygen species can be obtained from the ^{13}C NMR spectrum of the compound. It reveals 11 signals between 61 and 77 ppm which correspond to the sp^3-hybridized carbons of the fullerene core, where the hydroxyl groups are attached to, and 5 signals between 110 and 130 ppm which correspond to the vinyl ether species. To ensure the identity and purity of the compound, liquid chromatography was performed. It shows three very narrow signals with a similar retention time (shown in the Supporting Information, Figure S7). These signals represent the different number of oxygen species and confirm that no broad distribution nor a mixture of other compounds but a narrow distribution of oxygen species is present. It is also confirmed that no species with different chain numbers exist. Conclusively, one can say that precursor (**3**) was successfully polyhydroxylated with about 10 hemiketal moieties (which consist of a hydroxyl group and a vinyl ether group), resulting in an average of 20 oxygen species in total. It can be concluded that because of the inevitable characteristics of the poly-hydroxylation chemistry of fullerenes (see, for instance, the overview given by Wang et al.),[39] we are not dealing with a monomolecular species but rather with a system. In addition, the occurrence of regioisomers cannot be excluded. However, from all we can say is that there is a narrow distribution among the compounds and that their behavior is very similar.

It is important to note one further twist in the chemistry of fullerenols. It has been shown in the literature that the addition of acids leads to the conversion of hemiketals to ketones and hydroxyl groups accompanied by partial ring opening.[34,35] These reactions can be transferred successfully to our fullerenol surfactant, leading to the open-cage (oc) compound (**4oc**) (see the schematic Schlegel diagram shown in the Supporting Information, Figure S8). The FT-IR of (**4oc**) no longer shows the hemiketal signal but a strong ketone signal at 1720 cm^{-1} and 10 new ^{13}C NMR signals between 170 and 175 ppm, which are also characteristic for the presence of carbonyl units (see the Supporting Information, Figures S9 and S10). The number of ketone moieties perfectly fits the results obtained for the number of hemiketals in (**4cc**). Also, because of the complexity of the ring-opening processes (see also Figure S8), it is important to note that (**4oc**) does not represent a single molecular species but rather a range of compounds. In agreement with the literature, we also observed that the process is entirely reversible. The reformation of the molecule with its closed cage head group (**4cc**) can be achieved by the addition of diluted sodium hydroxide solution to (**4oc**).

Interfacial Properties and Self-Assembly. A first indication for the surfactant properties of (**4**) is that it forms strong foams at the air/water interface even at a low concentration (Figure 2). Further information can be obtained from concentration-dependent surface tension (γ) measurements shown in Figure 2.

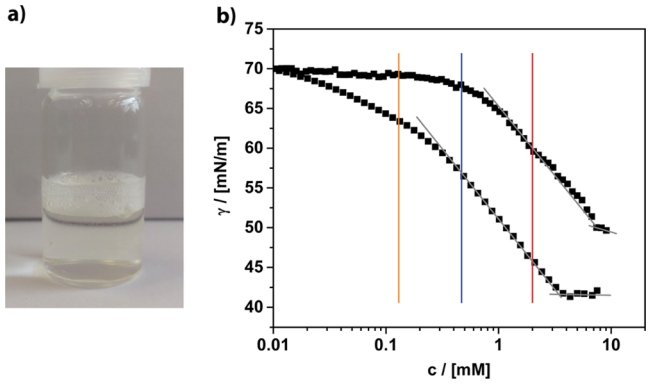

Figure 2. (a) Photograph of a diluted solution of the fullerenol surfactant indicating its foaming abilities. (b) Concentration-dependent surface tension measurements of (**4cc**) ≅ circles and (**4oc**) ≅ squares in water. The vertical bars indicate the concentrations whose particle size distribution curves are shown in Figure 3.

Compound (**4**) is obviously surface-active, but compared to classical nonionic surfactants such as Brij or Tween, there are differences. The behavior is more comparable to lipids.[40,41] The surface tension γ drops more slowly and does not reach such low values as for classical surfactants ($\gamma_{c=sat}$(Brij) ≈ 32 mN/m), and the concentration, at which γ begins to saturate, is roughly 1 magnitude higher [c_s(Brij 35) = 0.09 mM]. A possible explanation for the latter could be a less dense coverage of the air/water interface because of the large size of the head group in (**4**). This assumption can be confirmed by the calculation of the surface excess Γ and the minimum area per molecule at the air/water interface (A_m ≈ 60 $Å^2$), which represents a rather large value. The corresponding radius r_m = 0.44 nm fits very well to the cross section of the surfactant molecule (Figure 1b). One can also see that the chemical structure of the head has a marked influence on the surfactant properties. The overall performance of the (**4oc**) system seems to be better; the surfactant is more soluble and occupies the air/water interface at a lower concentration compared to (**4cc**).

Micelles are usually formed above the critical micelle concentration (cmc), which is reached as soon as the air/water interface is fully occupied. Therefore, at none of the three concentrations marked in Figure 2, one should expect to find aggregates in solution. We checked this by dynamic light scattering (DLS) shown in Figure 3a. However, already at c ≈

DOI: 10.1021/acsami.8b07032
ACS Appl. Mater. Interfaces 2018, 10, 23638−23646

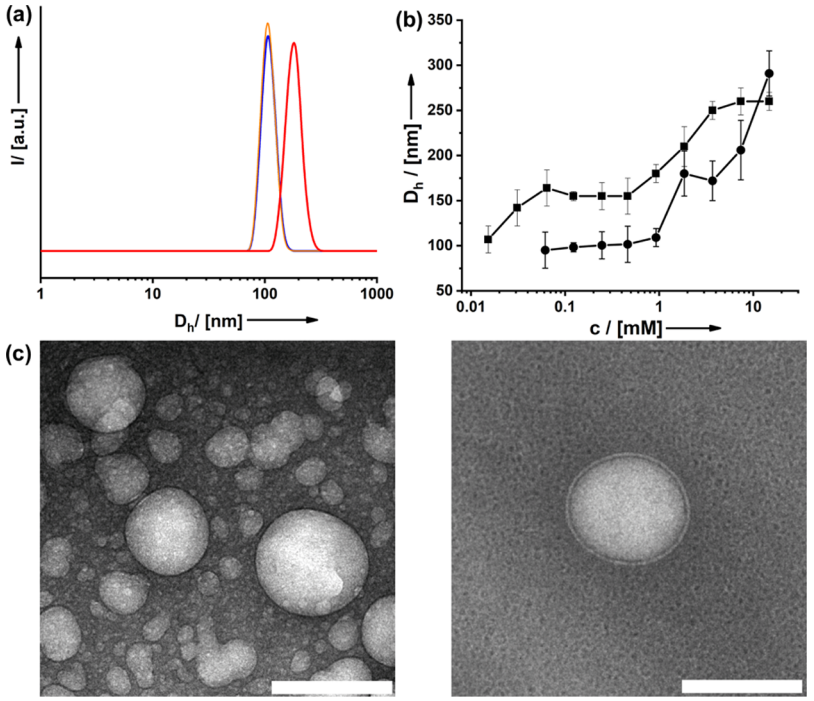

Figure 3. (a) Particle size distribution functions derived from DLS for the three concentrations of (**4cc**) given in Figure 2. (b) Aggregate size in water at different surfactant concentrations of (**4cc**) ≅ circles and (**4oc**) ≅ squares. (c) Cryo-TEM micrographs of aggregates in solution; scale bar = 100 nm.

0.1 mM, one observes large aggregates, although γ has just begun to drop, and thus, the air/water interface is covered only partially. The absence of a classic cmc was confirmed by independent methods (concentration-dependent viscosity and ionic conductivity measurements; see the Supporting Information, Figure S11). We suppose that the packing of (**4**) at the air/water interface is so ineffective that it is thermodynamically more favorable to form aggregates even at very low concentration. Interestingly, Nakamura and co-workers observed that for an alternative amphiphilic fullerene system, aggregate formation is possible without interaction with the air/water interface.[24] Even at much lower concentration, we never saw the formation of micelles but large aggregates with ($D_H \approx 100$ nm) even at ≈20 μM. The concentration of the aggregates becomes lower, until they vanish. The particle size ($D_H \approx 100/150$ nm) remains unchanged in the concentration range 0.1−2 mM and then raises until the solution is saturated (Figure 2b). As a consequence, the optical appearance of the dispersions has become turbid (see also the Supporting Information, Figure S12).

The mentioned aggregates are obviously much larger than the ordinary micelles, which are typically only twice the length of the surfactant. Because the packing parameter of (**4**) is close to 1, one can expect a tendency for the formation of bilayered or vesicle-like structures. Other researchers working on amphiphilic fullerenes could also observe vesicle-like structures.[19,23,42,43] Investigations using cryogenic transmission electron microscopy (cryo-TEM) confirm this (Figure 3c). The size of the hollow aggregates is in agreement with the DLS data. One has to bear in mind that DLS is an averaging technique, and one preferentially sees only the strongest light scatters, for example, the larger aggregates. Actually, the size of the vesicles is not monodisperse at all (Figure 3c). Additional TEM data are given in the Supporting Information (Figure S12). It can also be seen that with higher concentration, more and more vesicles form, and they seem to be fusing together, which is the reason for the increasing aggregate size observed in DLS. Similar processes have also been reported in the literature for other surfactant systems, for example, cetyltrimethylammonium bromide.[44,45] The TEM data reveal that the vesicles contain a single shell. The thickness of this shell (∼4.8 nm) is compliant with the double dimension of the fullerenol surfactant (Figure 1b) and, thus, fits a double-layer structure. Although both surfactant types (**4cc**) and (**4oc**) form vesicles, one can see that the chemical conformation of the head groups has an influence on the average size of the aggregates (Figure 3b). At higher concentration, liquid-crystalline phases can be observed. Optical microscopy under crossed polarizers shows phases with intense birefringence and marked textures (see the Supporting Information, Figure S13). Depending on the surfactant concentration, one observes columnar droplets with the characteristic Maltese cross or smectic phases.

Ex Vivo ROS Quenching. The antioxidative properties and the influence of the amphiphilic character are investigated next. Quenching of superoxide monitored by a nitroblue tetrazolium assay (see the Supporting Information, Figure S14)[46] was used to evaluate the efficiency of the fullerenol surfactants at different concentrations (Figure 4). The results were compared to two reference systems: a nonamphiphilic fullerenol compound, synthesized by hydroxylation of $C_{60}Br_{24}$,[47] and the flavonoid quercetin which was employed as a benchmark because it is a commercially available and well-understood antioxidant.[9−11,32,48] The nonamphiphilic fullerenol is active in superoxide quenching, as described in the literature. The quenching efficiency depends almost linearly on the concentration of (**4cc**) (Figure 4). A substantial amount of superoxide (>60%) remains in solution even at a relatively high concentration of fullerenol. The 50% inhibitory concentration (IC_{50}) of this reference is not reached during our experiment.

DOI: 10.1021/acsami.8b07032
ACS Appl. Mater. Interfaces 2018, 10, 23638−23646

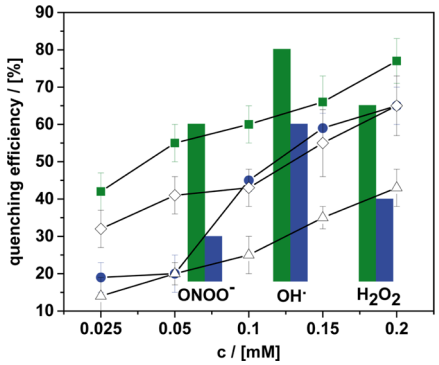

Figure 4. Concentration-dependent superoxide quenching efficiency of different compounds: (**4cc**) ≙ blue circles, (**4oc**) ≙ green squares, nonamphiphilic fullerenol (open triangles), and quercetin (open hashes). The bars give an overview over the ROS quenching capabilities of (**4cc**) (blue) and (**4oc**) (green) for $ONOO^-$, $OH^•$, and H_2O_2 as the alternative ROS (see the Supporting Information for method details).

The surfactant containing fullerenol as a head group (**4cc**) clearly shows an improved performance. The IC_{50} of (**4cc**) is 0.15 mM. One sees that there is a jump in the quenching efficiency between 0.05 and 0.1 mM surfactant concentration. Because this is the same region, where the (**4cc**) vesicles are formed (see Figure 3a), the step can be seen as an indication; the presence of the vesicles is very important. The fraction of the fullerenol entities exposed to the aqueous interface is obviously maximized for the vesicles, and therefore, the superoxide quenching ability is much better.

The vesicles containing (**4cc**) are just as efficient as the benchmark quercetin (Figure 4) but unfortunately not better. Because (**4oc**) forms vesicles at much lower concentration (Figure 3a), we hoped that it could exhibit higher quenching efficiency in particular at those low concentrations. This is indeed the case as can be seen from Figure 4. Compound (**4oc**) does outperform (**4cc**) and, more importantly, quercetin. Since this is also the case for higher concentrations, one can assume that more than the tendency to form vesicles is a relevant factor. Because the vesicles of (**4oc**) are larger than those formed by (**4cc**) (Figure 3), the explanation cannot be due to an improved surface-to-volume ratio, which could result in an increased catalytic conversion rate of superoxide. Therefore, the chemical structure of the head group in (**4oc**) must be relevant; in particular, the ketone moieties play a crucial role regarding the ROS deactivation mechanism (see the Supporting Information, Figure S15). Besides the superoxide ion ($O_2^{•-}$), other ROS were investigated as well, such as peroxynitrite ($ONOO^-$), hydroxyl radicals ($OH^•$), and hydrogen peroxide (H_2O_2).[49] For the other ROS, the surfactants also quenched the radical species reliably (Figure S16), and (**4oc**) was in all cases superior than (**4cc**). The activity regarding the catalytic conversion of H_2O_2 is a positive result. According to the literature, H_2O_2 is the main product of the deactivation process of superoxide.[32] Of course, H_2O_2 is still quite reactive and a strong oxidant. Because the surfactants (**4**) lead to a decrease in H_2O_2 concentration, we expect an even more significant improvement in the oxidative stress level.

Biocompatibility and in Vivo ROS Quenching. Before a beneficial biological function of (**4**) can be explored, it is pivotal to scrutinize any potential toxicity factors. Although nonnatural surfactants are in general not very toxic, they can be harmful, in particular, when they come in contact with more sensitive cells.[50−52] Therefore, we investigated the viability and morphology of a range of prokaryotic and eukaryotic cell types in contact to (**4**). *Pseudomonas aeruginosa* and *Escherichia coli* were chosen as prokaryotic model organisms. In comparison, the eukaryotic model systems human liver cells (HepG2) and human dopaminergic neurons (LUHMES) represent much more delicate systems. The intrinsic toxicity of the surfactants was tested in a range of 1−125 μM, according to standard procedures (see also the Supporting Information).

For *E. coli*, as well as for *P. aeruginosa* (not shown), the presence of the surfactant had no negative effects neither on their growth (see the Supporting Information, Figure S17) nor on their viability (Figure 5a). The viability of both, LUHMES

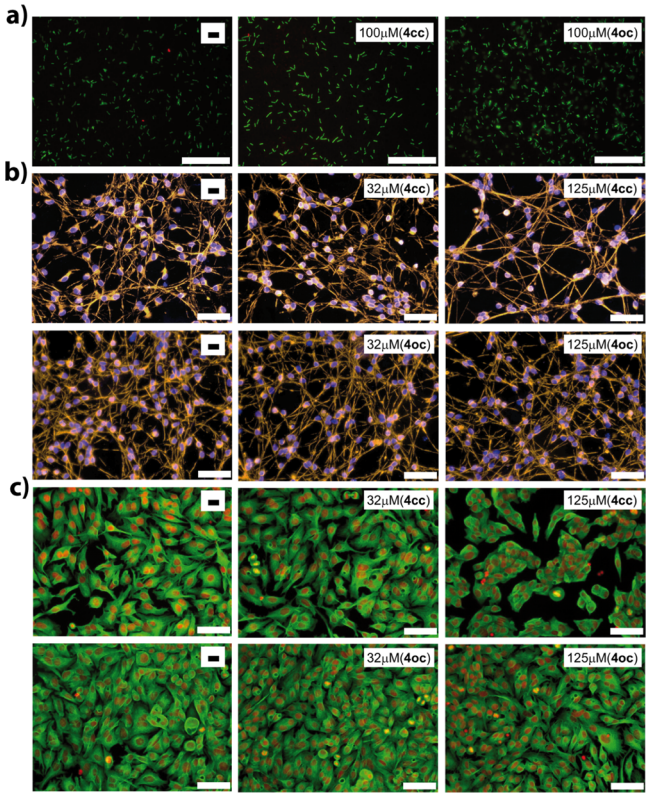

Figure 5. Live/dead stain images or morphology of different cells treated with (**4**). Blank experiments in the absence of any surfactant are always shown on the left. The concentration of the surfactant and the head group form is given in the white boxes. *E. coli* (a; scale bar = 20 μm), LUHMES neurons (b; scale bar = 100 μm), and HepG2 hepatoma cells (c; scale bar = 100 μm).

and HepG2, is also not influenced at a low concentration (32 μM) of the surfactant (Figure 5b,c). There is a minor effect at a higher concentration (125 μM), if compound (**4cc**) is used. Interestingly, the toxicity of (**4oc**) is so low; we cannot see any changes at the same concentration. The extraordinary biocompatibility of the surfactants was confirmed further by lactate dehydrogenase (LDH) release assay and resazurin metabolization assay (Figures S18−S21). Obviously, our fullerenol surfactants are harmless to both prokaryotic and eukaryotic cells in biologically relevant concentrations. Therefore, we can test now the possible antioxidative properties of the compounds in a cellular system (LUHMES). The cells were treated with the neurotoxicant 1-methyl-4-phenyl-

DOI: 10.1021/acsami.8b07032
ACS Appl. Mater. Interfaces 2018, 10, 23638−23646

pyridinium (MPP^+).[53] As expected, the viability of the cells is drastically reduced caused by MPP^+ (Figure 6). The situation

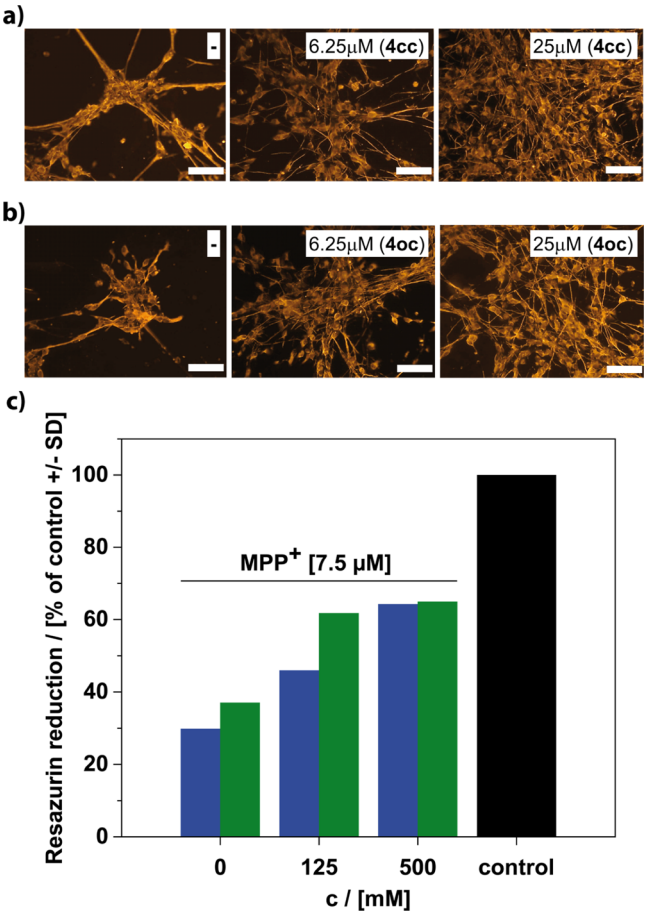

Figure 6. (a,b; scale bar = 100 μm) Morphology of eukaryotic LUHMES cell line treated with MPP^+ (7.5 μM) and surfactant (**4**). Blank experiments in the absence of any surfactant are always shown on the left. The concentration of the surfactant and the head group form is given in the white boxes. (c) Viability of LUHMES after the cells were loaded with the surfactant in the concentrations as indicated for a period of 3 h. Following the removal of the compounds in the supernatant by medium exchange, the toxicant MPP^+ (7.5 μM) was added for 60 h. Control cells received neither MPP^+ nor surfactant. Compound (**4cc**) blue bars and compound (**4oc**) green bars.

changed when the surfactant was present. Even low concentrations of (**4**) had a positive effect, and at 25 μM, the viability of the cells has increased significantly. The viability of the cells was again confirmed by LDH release assay and resazurin metabolization assay (Supporting Information, Figure S22). There are only minor differences comparing (**4cc**) and (**4oc**).

The final question remaining is that if the protection against oxidative stress is due to surfactants and their vesicle present in the outer medium or if the cells do actually include the surfactants into their cell membrane. The treatment of cells with the surfactant is a standard procedure in cell biology. We have followed similar protocols (see Methods section), but the surfactant concentration was low enough to avoid lysis. Furthermore, we have exposed LUHMES to a surfactant solution containing different concentrations of (**4**) only for 3 h. This short time was sufficient; a notable decrease of concentration in the mother liquor could be detected. The cells were then separated from the supernatant solvent and washed. It was made sure that there is no surfactant anymore in the external medium. Finally, the cells were then treated with MPP^+ for 60 h. If the surfactant had just been present in the external medium, we should not expect any protection anymore and in particular no concentration dependence. Figure 6c shows the results of the assessment of resazurin reduction assay; there still remains significant protection, which scales with the concentration of the surfactant used in the original solution. This allows only one conclusion. LUHMES cells have integrated with the fullerenol surfactant, and this way, they could decrease the stress level significantly. It is important to mention that the interaction of the surfactants with cells has already been studied multiple times by others in the past.[54−56] It could be proven that certain amphiphiles do interact with cellular membranes and become incorporated. Therefore, we have followed similar protocols. Therefore, it is not surprising that the fullerenol surfactant behaves similar.

CONCLUSIONS

On the basis of the encouraging findings about potential biotechnological applications of fullerene derivatives in the literature, we prepared a defined surfactant species containing a polyhydroxylated C_{60}, a fullerenol, as the hydrophilic head group. The necessary Janus-type modification of the fullerene was accomplished by attaching five alkyl chains on one side of C_{60} first, followed by modification with an average of 20 oxygen species consisting of hemiketals for compound **4cc** and ketones and hydroxyl groups for compound **4oc** on the other side. Caused by the packing parameter close to 1, the surfactant showed features similar to natural surfactants (lipids). There is a high tendency for the formation of vesicle-like structures in water, and at higher concentration lyotropic liquid crystals with lamellar characteristics have been observed.

Because of the fullerenol head group, the surfactant obtained an added functionality, the catalytic deactivation of ROS-like superoxide, peroxynitrite, hydroxyl radicals, and even hydrogen peroxide. Because the surfactants are fully biocompatible and benign even against delicate cells such as human liver cells (HepG2) and human dopaminergic neurons (LUHMES), we could explore the in vivo application for the reduction of oxidative stress. It was shown that the cells do actually integrate the surfactants. The lipid-like character and the high activity in ROS quenching in the cells indicate that the cells implement the fullerenol surfactants into their cellular membranes.

We have also seen that the fullerenol head group can exist in two alternative forms, which can be reversibly converted into each other by acid/base treatment. The form of the head group had a marked effect on all surfactant properties, including self-assembly and ROS quenching behavior. The surfactant containing the open-cluster form (**4oc**) seems to be superior overall.

METHODS

General Information. The synthesis that acquired inert gas atmosphere was performed using general Schlenk techniques under argon atmosphere. The solvents were dried according to the standard literature and stored under argon. Water was deionized with Millipore Milli-Q. All starting materials used for the synthesis were purchased

DOI: 10.1021/acsami.8b07032
ACS Appl. Mater. Interfaces 2018, 10, 23638−23646

from commercial sources unless stated differently. The fullerene C_{60} (pur. 99.9%) was purchased from SES research.

Synthesis of Hexachlorofullerene ($C_{60}Cl_6$) (2). C_{60} (0.28 mmol) was dissolved in chlorobenzene (11 mL) and sonicated for 5 min. Iodine monochloride (6.95 mmol) was added in one shot, and the solvent was evaporated at 35 °C. The crude product was further purified by column chromatography (silica gel, eluent: toluene). $C_{60}Cl_6$ is obtained as a red solid (0.2 mmol, 70%).

Synthesis of Penta-Alkylated Fullerene ($C_{60}R_5Cl$) (3). $C_{60}Cl_6$ (0.28 mmol) was dissolved in dry toluene (30 mL) and vigorously stirred. Dodecylamine (2.52 mmol) and potassium carbonate (1 g) were added. The mixture was stirred for 12 h. The solvent was evaporated under reduced pressure. The obtained solid was suspended in methanol, filtrated, and washed three times with methanol. The crude product was obtained by washing with ethyl acetate. The solvent was evaporated, and the crude product was further purified by column chromatography (silica gel, eluent: toluene/EE). The title compound is obtained as a red solid (0.17 mmol, 60%).

IR (powder): 3285, 2920, 2851, 1770, 1658, 1570, 1466, 1316, 1115 cm^{-1}; ^1H NMR (400 MHz, $CDCl_3$): δ 0.89 (t, ^3J = 7.2 Hz, 15H), 1.27 (m, 90H), 1.45 (m, 10H), 1.67 (m, 10H), 3.22 (m, 5H); ^{13}C NMR (100 MHz, $CDCl_3$): δ 22.56, 27.57, 27.67, 29.56, 29.58, 29.91, 29.93, 30.95, 31.02, 32.11, 47.36, 47.87, 47.88, 66.02, 68.21, 69.35, 143.24, 143.31, 143.71, 143.81, 143.83, 143.84, 143.84, 143.88, 144.02, 144.08, 144.31, 144.47, 144.51, 144.53, 144.91, 145.43, 147.16, 147.21, 147.23, 147.29, 147.62, 148.02, 148.21, 148.33, 148.57, 148.71, 149.12, 150.81, 153.88, 155.31; MS (MALDI): 1641.6 $[M - HCl]^-$, 1506.2 $[M - C_{12}H_{26}]^-$, 1457.1 $[M - C_{12}H_{25} - Cl]^-$, 1337.9 $[M - C_{24}H_{51}]^-$, 1307.0 $[M - N_2C_{24}H_{54}]^-$, 1272.8, 1307.0 $[M - N_2C_{24}H_{54} - Cl]^-$, 1167.6 $[M - C_{36}H_{76}]^-$, 1152.5 $[M - NC_{36}H_{77}]^-$, 1137.5 $[M - N_2C_{36}H_{78}]^-$, 1122.5 $[M - N_3C_{36}H_{79}]^-$, 1087.3 $[M - N_3C_{36}H_{79} - Cl]^-$.

Synthesis of the Polyhydroxylated Penta-Alkylated Fullerene Surfactant (4cc). $C_{60}Cl(HNC_{12}H_{25})_5$ (0.15 mmol) was dissolved in tetrahydrofuran (THF) (8 mL) and sonicated for 10 min. Solid NaOH (0.3 g) was added, and H_2O_2 (15 mL) was added under vigorous stirring. The mixture was heated to reflux for 4 h until a yellow solution is formed. THF was evaporated under reduced pressure, and the mixture was filtrated to remove nonwater-soluble compounds. Afterward, the volume of the solution was reduced to about 3 mL, and the reaction was cooled to room temperature. Methanol was added, and the product was precipitated. The precipitate was stirred in diluted NaOH for 5 min, and the solvent was evaporated. The crude product was washed five times with methanol to remove the remaining NaOH. The product is obtained as a light yellow-brown solid with an average number of 20 oxygen species (0.075 mmol, 50%). For characterization data, see the Supporting Information.

Conversion to the Open-Cage Compound (4oc). Compound (**4**) was dissolved in diluted hydrochloric acid and stirred for 10 min. The solvent was evaporated, and the product was obtained as a yellow oily solid. For characterization data, see the Supporting Information.

Biological Experiments. *Treatment of Cells with the Surfactant.* In a first step, the cells were grown under standard conditions as described in Figure S18. The cell culture plates were coated with 50 poly-L-ornithine and fibronectin overnight at 37 °C and washed two times with water. Cells were propagated in advanced Dulbecco's modified Eagle's medium (DMEM)/F12, 1× N_2 supplement, 2 mM L-glutamine (Gibco), and 40 ng/mL recombinant bFGF (R + D Systems; Minneapolis, MN). The differentiation process was initiated by the addition of differentiation medium consisting of advanced DMEM/F12, 1× N_2 supplement, 2 mM L-glutamine, 1 mM dibutyryl-cAMP, 1 μg/mL tetracycline, and 2 ng/mL recombinant human GDNF (R + D Systems). After 2 days, cells were trypsinized and collected in advanced DMEM/F12 medium. Cells were seeded onto 96-well plates at a density of 35 000 cells/well. The differentiation process was continued for additional 3 days. After the growing and differentiation process, the cells were treated with different surfactant concentrations for 3 h. During this time, the surfactant molecules could interact with the cell membranes. After that process, the medium was changed and washed several times, so all remaining surfactant molecules that are not incorporated into the cell wall are removed from the system. With these prepared cells, the experiments were performed. These cells were then treated with MPP^+. After an incubation time of 60 h, resazurin metabolization assay and LDH release assay have been performed.

Live/Dead Stain E. coli Treated with the Surfactant. Live/dead staining is performed by following the manufacturer's instructions (LIVE/DEAD BacLight Bacterial Viability Kit, Thermofisher); it stains cells with membrane damage in red, against viable cells stained in green. The stained cells were placed on agar-coated microscopic slides and observed under a fluorescence microscope at 400-fold magnification.

Morphology of LUHMES Treated with the Surfactant. For visualization of cell morphology, the cells were fixed with 4% paraformaldehyde for 20 min at room temperature (RT), permeabilized with 0.2% Triton X-100, washed, and blocked with 1% bovine serum albumin (BSA; Calbiochem, San Diego, CA) in phosphate-buffered saline (PBS) for 1 h. LUHMES were stained with an anti-β-III-tubulin antibody (rabbit, Sigma, 1:1000) in 1% BSA/PBS at 4 °C overnight. After washing, the secondary antibodies were added for 1 h, and nuclei were stained by Hoechst H-33342 (1 μg/mL) for 20 min. For quantitative evaluation of the neurite area, live staining of LUHMES was conducted with calcein-AM (1 μM) and Hoechst H-33342 (1 μg/mL) for 30 min. Images were collected by an automated microplate-reading microscope (Array-Scan II HCS Reader, Cellomics, Pittsburgh, PA) equipped with a Hamamatsu ORCA-ER camera (resolution 1024 × 1024; run at 2 × 2 binning) in two different fluorescence channels. Nuclei were identified as objects according to their intensity, size, area, and shape. A virtual area corresponding to the cell soma was defined around each nucleus. The total calcein pixel area per field minus the soma areas in that field was defined as the neurite mass. In addition, viability was analyzed by the detection of the percentage of those cells positive for calcein and for H-33342.

Morphology of HepG2 Treated with the Surfactant. For visualization of cell morphology, the cells were fixed with 4% paraformaldehyde for 20 min at RT, permeabilized with 0.2% Triton X-100, washed, and blocked with 1% BSA (Calbiochem, San Diego, CA) in PBS for 1 h. HepG2 cells were stained with a monoclonal anti-α-tubulin antibody (Sigma; 1:1000).

Resazurin Metabolization Assay and LDH Release Assay. Resazurin metabolization assay: Resazurin (Sigma) was added to the cell culture medium in a final concentration of 5 μg/mL and fluorescence was measured after 60 min (λ_{ex} = 530 nm; λ_{em} = 590 nm). LDH release assay: The LDH activity was detected separately in the supernatant and cell lysate. Following the separation of the supernatants, the cells were lysed in PBS/0.5% Triton X-100 for >60 min. The percentage of LDH released was calculated as 100 × $LDH_{supernatant}/LDH_{supernatant+lysate}$. For the enzymatic assay, 20 μL of the sample was combined with 180 μL of the reaction buffer containing NADH (100 μM) and sodium pyruvate (600 μM) in sodium phosphate buffer adjusted to pH 7.4 by titration with K_2HPO_4 (40 mM) and KH_2PO_4 (10 mM). Absorption at 340 nm was detected at 37 °C in 1 min intervals over a period of 20 min, and the enzyme activity was calculated from the respective slopes.

Analytical Methods. NMR measurements (^1H, ^{13}C) were performed on a Varian INOVA 400 MHz spectrometer. MALDI-MS measurements were performed using a Bruker Microflex MALDI-TOF. The samples were prepared in a cyano-4-hydroxycinnamic acid matrix or a *trans*-2-[3-(4-*tert*-butylphenyl)-2-methyl-2-propenylidene]malononitrile matrix. Attenuated total reflection–infrared (ATR–IR) spectra were measured with a Perkin Elmer 100 Spectrum spectrometer including an ATR unit. TGA was measured at Netzsch Jupiter STA 449 F3. Liquid chromatography was measured with Thermo Fisher Scientific Dionex 3000. As the column, Agilent Poroshell 120 EC-C18 (2.1 × 100 mm, 2.7 μm) was used. MeCN (5%) as eluent A and 95% water as eluent B with 0.1% formic acid were used. A linear gradient of 5% A to 100% A was applied with

DOI: 10.1021/acsami.8b07032
ACS Appl. Mater. Interfaces 2018, 10, 23638–23646

a flow rate of 0.3 mL/min. The DLS measurements were done by using a Malvern Zen5600. Liquid-crystal pictures were taken with an Olympus CX41 light microscope. The high-resolution TEM observations were carried out using JEOL JEM-2200FS, and the TEM observations were carried out using Zeiss Libra120. The surface tension measurements were performed using Krüss K100.

■ ASSOCIATED CONTENT

Supporting Information

The Supporting Information is available free of charge on the ACS Publications website at DOI: 10.1021/acsami.8b07032.

Supporting molecular characterization and details regarding biological experiments (PDF)

■ AUTHOR INFORMATION

Corresponding Author

*E-mail: sebastian.polarz@uni-konstanz.de.

ORCID

Klaus Boldt: 0000-0002-0035-2490

Sebastian Polarz: 0000-0003-1651-4906

Author Contributions

The manuscript was written through contributions from all authors. All authors have given approval to the final version of the manuscript.

Notes

The authors declare no competing financial interest.

■ ACKNOWLEDGMENTS

The current research was funded by an ERC consolidator grant (I-SURF; project 614606). K.B. is thankful for the financial support from the Fonds der Chemischen Industrie through a Liebig Fellowship and by the Zukunftskolleg Konstanz through a 5-year Marie Curie ZIF Research Fellowship. European Research Council Fonds der Chemischen Industrie.

■ REFERENCES

(1) Prather, K. L. J.; Martin, C. H. De novo biosynthetic pathways: rational design of microbial chemical factories. *Curr. Opin. Biotechnol.* **2008**, *19*, 468−474.

(2) Adkins, J.; Pugh, S.; McKenna, R.; Nielsen, D. R. Engineering microbial chemical factories to produce renewable biomonomers. *Front. Microbiol.* **2012**, *3*, 313.

(3) Finkel, T.; Holbrook, N. J. Oxidants, oxidative stress and the biology of ageing. *Nature* **2000**, *408*, 239−247.

(4) Circu, M. L.; Aw, T. Y. Reactive oxygen species, cellular redox systems, and apoptosis. *Free Radical Biol. Med.* **2010**, *48*, 749−762.

(5) Ott, M.; Gogvadze, V.; Orrenius, S.; Zhivotovsky, B. Mitochondria, oxidative stress and cell death. *Apoptosis* **2007**, *12*, 913−922.

(6) Chiang, L. Y.; Lu, F.-J.; Lin, J.-T. Free radical scavenging activity of water-soluble fullerenols. *J. Chem. Soc., Chem. Commun.* **1995**, 1283−1284.

(7) Yin, J.-J.; Lao, F.; Fu, P. P.; Wamer, W. G.; Zhao, Y.; Wang, P. C.; Qiu, Y.; Sun, B.; Xing, G.; Dong, J.; Liang, X.-J.; Chen, C. The scavenging of reactive oxygen species and the potential for cell protection by functionalized fullerene materials. *Biomaterials* **2009**, *30*, 611−621.

(8) Chiang, L. Y.; Bhonsle, J. B.; Wang, L.; Shu, S. F.; Chang, T. M.; Hwu, J. R. Efficient one-flask synthesis of water-soluble [60]-fullerenols. *Tetrahedron* **1996**, *52*, 4963−4972.

(9) Yin, J.-J.; Lao, F.; Fu, P. P.; Wamer, W. G.; Zhao, Y.; Wang, P. C.; Qiu, Y.; Sun, B.; Xing, G.; Dong, J.; Liang, X.-J.; Chen, C. The scavenging of reactive oxygen species and the potential for cell protection by functionalized fullerene materials. *Biomaterials* **2009**, *30*, 611−621.

(10) Markovic, Z.; Trajkovic, V. Biomedical potential of the reactive oxygen species generation and quenching by fullerenes (C60). *Biomaterials* **2008**, *29*, 3561−3573.

(11) Partha, R.; Conyers, J. L. Biomedical applications of functionalized fullerene-based nanomaterials. *Int. J. Nanomed.* **2009**, *4*, 261−275.

(12) Djordjević, A.; Bogdanović, G.; Dobrić, S. Fullerenes in biomedicine. *J. BUON* **2006**, *11*, 391−404.

(13) Nakamura, H.; Nozaki, Y.; Koizumi, Y.; Watano, S. Effect of number of hydroxyl groups of fullerenol C60(OH)n on its interaction with cell membrane. *J. Taiwan Inst. Chem. Eng.* **2017**, DOI: 10.1016/j.jtice.2017.11.016.

(14) Guldi, D. M.; Zerbetto, F.; Georgakilas, V.; Prato, M. Ordering Fullerene Materials at Nanometer Dimensions. *Acc. Chem. Res.* **2005**, *38*, 38−43.

(15) Yu, X.; Li, Y.; Dong, X.-H.; Yue, K.; Lin, Z.; Feng, X.; Huang, M.; Zhang, W.-B.; Cheng, S. Z. D. Giant Surfactants Based on Molecular Nanoparticles: Precise Synthesis and Solution Self-assembly. *J. Polym. Sci., Part B: Polym. Phys.* **2014**, *52*, 1309−1325.

(16) Burger, C.; Hao, J.; Ying, Q.; Isobe, H.; Sawamura, M.; Nakamura, E.; Chu, B. Multilayer vesicles and vesicle clusters formed by the fullerene-based surfactant C60(CH3)5K. *J. Colloid Interface Sci.* **2004**, *275*, 632−641.

(17) Sano, M.; Oishi, K.; Ishi-i, T.; Shinkai, S. Vesicle Formation and Its Fractal Distribution by Bola-Amphiphilic [60]Fullerene. *Langmuir* **2000**, *16*, 3773−3776.

(18) Cassell, A. M.; Asplund, C. L.; Tour, J. M. Self-Assembling Supramolecular Nanostructures from a C60 Derivative: Nanorods and Vesicles. *Angew. Chem., Int. Ed.* **1999**, *38*, 2403−2405.

(19) Homma, T.; Harano, K.; Isobe, H.; Nakamura, E. Preparation and properties of vesicles made of nonpolar/polar/nonpolar fullerene amphiphiles. *J. Am. Chem. Soc.* **2011**, *133*, 6364−6370.

(20) Zhao, Y. M.; Chen, G. C-60 Fullerene Amphiphiles as Supramolecular Building Blocks for Organized and Well-Defined Nanoscale Objects. In *Fullerenes and Other Carbon-rich Nanostructures*; Nierengarten, J. F., Ed.; Springer-Verlag Berlin: Berlin, 2014; Vol. *159*, pp 23−53.

(21) Partha, R.; Mitchell, L. R.; Lyon, J. L.; Joshi, P. P.; Conyers, J. L. Buckysomes: fullerene-based nanocarriers for hydrophobic molecule delivery. *ACS Nano* **2008**, *2*, 1950−1958.

(22) Brettreich, M.; Burghardt, S.; Böttcher, C.; Bayerl, T.; Bayerl, S.; Hirsch, A. Globular Amphiphiles: Membrane-Forming Hexaadducts of C60. *Angew. Chem., Int. Ed.* **2000**, *39*, 1845−1848.

(23) Partha, R.; Lackey, M.; Hirsch, A.; Casscells, S. W.; Conyers, J. L. Self assembly of amphiphilic C60 fullerene derivatives into nanoscale supramolecular structures. *J. Nanobiotechnol.* **2007**, *5*, 6.

(24) Nitta, H.; Harano, K.; Isomura, M.; Backus, E. H. G.; Bonn, M.; Nakamura, E. Conical Ionic Amphiphiles Endowed with Micellization Ability but Lacking Air-Water and Oil-Water Interfacial Activity. *J. Am. Chem. Soc.* **2017**, *139*, 7677−7680.

(25) Lin, Z.; Lu, P.; Hsu, C.-H.; Yue, K.; Dong, X.-H.; Liu, H.; Guo, K.; Wesdemiotis, C.; Zhang, W.-B.; Yu, X.; Cheng, S. Z. D. Self-Assembly of Fullerene-Based Janus Particles in Solution: Effects of Molecular Architecture and Solvent. *Chem.—Eur. J.* **2014**, *20*, 11630−11635.

(26) Chen, M.; Zhu, H.; Zhou, S.; Xu, W.; Dong, S.; Li, H.; Hao, J. Self-Organization and Vesicle Formation of Amphiphilic Fulleromonodendrons Bearing Oligo(poly(ethylene oxide)) Chains. *Langmuir* **2016**, *32*, 2338−2347.

(27) Burghardt, S.; Hirsch, A.; Schade, B.; Ludwig, K.; Böttcher, C. Switchable supramolecular organization of structurally defined micelles based on an amphiphilic fullerene. *Angew. Chem., Int. Ed.* **2005**, *44*, 2976−2979.

(28) Donskyi, I.; Achazi, K.; Wycisk, V.; Böttcher, C.; Adeli, M. Synthesis, self-assembly, and photocrosslinking of fullerene-polyglycerol amphiphiles as nanocarriers with controlled transport properties. *Chem. Commun.* **2016**, *52*, 4373−4376.

(29) Kuvychko, I. V.; Streletskii, A. V.; Popov, A. A.; Kotsiris, S. G.; Drewello, T.; Strauss, S. H.; Boltalina, O. V. Seven-Minute Synthesis of Pure Cs-C60Cl6 from [60] Fullerene and Iodine Monochloride: First IR, Raman, and Mass Spectra of 99 mol% C60Cl6. *Chem.—Eur. J.* **2005**, *11*, 5426−5436.
(30) Kornev, A. B.; Khakina, E. A.; Troyanov, S. I.; Kushch, A. A.; Peregudov, A.; Vasilchenko, A.; Deryabin, D. G.; Martynenko, V. M.; Troshin, P. A. Facile preparation of amine and amino acid adducts of [60]fullerene using chlorofullerene C60Cl6 as a precursor. *Chem. Commun.* **2012**, *48*, 5461−5463.
(31) Wang, S.; He, P.; Zhang, J.-M.; Jiang, H.; Zhu, S.-Z. Novel and Efficient Synthesis of Water-Soluble [60]Fullerenol by Solvent-Free Reaction. *Synth. Commun.* **2005**, *35*, 1803−1808.
(32) Wang, Z.; Wang, S.; Lu, Z.; Gao, X. Syntheses, structures and antioxidant activities of fullerenols: knowledge learned at the atomistic level. *J. Cluster Sci.* **2015**, *26*, 375−388.
(33) Kokubo, K.; Shirakawa, S.; Kobayashi, N.; Aoshima, H.; Oshima, T. Facile and scalable synthesis of a highly hydroxylated water-soluble fullerenol as a single nanoparticle. *Nano Res.* **2011**, *4*, 204−215.
(34) Xing, G.; Zhang, J.; Zhao, Y.; Tang, J.; Zhang, B.; Gao, X.; Yuan, H.; Qu, L.; Cao, W.; Chai, Z.; Ibrahim, K.; Su, R. Influences of structural properties on stability of fullerenols. *J. Phys. Chem. B* **2004**, *108*, 11473−11479.
(35) Chiang, L. Y.; Upasani, R. B.; Swirczewski, J. W.; Soled, S. Evidence of hemiketals incorporated in the structure of fullerols derived from aqueous acid chemistry. *J. Am. Chem. Soc.* **1993**, *115*, 5453−5457.
(36) Afreen, S.; Kokubo, K.; Muthoosamy, K.; Manickam, S. Hydration or hydroxylation: direct synthesis of fullerenol from pristine fullerene [C60] via acoustic cavitation in the presence of hydrogen peroxide. *RSC Adv.* **2017**, *7*, 31930−31939.
(37) Semenov, K. N.; Letenko, D. G.; Charykov, N. A.; Nikitin, V. A.; Matuzenko, M. Y.; Keskinov, V. A.; Postnov, V. N.; Kopyrin, A. A. Synthesis and identification of fullerenol prepared by the direct oxidation route. *Russ. J. Appl. Chem.* **2010**, *83*, 2076−2080.
(38) Chao, T.-C.; Song, G.; Hansmeier, N.; Westerhoff, P.; Herckes, P.; Halden, R. U. Characterization and liquid chromatography-MS/MS based quantification of hydroxylated fullerenes. *Anal. Chem.* **2011**, *83*, 1777−1783.
(39) Wang, Z.; Lu, Z.; Zhao, Y.; Gao, X. Oxidation-induced water-solubilization and chemical functionalization of fullerenes C60, Gd@C60and Gd@C82: atomistic insights into the formation mechanisms and structures of fullerenols synthesized by different methods. *Nanoscale* **2015**, *7*, 2914−2925.
(40) McConnell, H. M. Structures And Transitions In Lipid Monolayers At The Air-Water Interface. *Annu. Rev. Phys. Chem.* **1991**, *42*, 171−195.
(41) Egberts, J.; Sloot, H.; Mazure, A. Minimal surface tension, squeeze-out and transition temperatures of binary mixtures of dipalmitoylphosphatidylcholine and unsaturated phospholipids. *Biochim. Biophys. Acta* **1989**, *1002*, 109−113.
(42) Lin, M.-S.; Chen, R.-T.; Yu, N.-Y.; Sun, L.-C.; Liu, Y.; Cui, C.-H.; Xie, S.-Y.; Huang, R.-B.; Zheng, L.-S. Fullerene-based amino acid ester chlorides self-assembled as spherical nano-vesicles for drug delayed release. *Colloids Surf., B* **2017**, *159*, 613.
(43) Burger, C.; Hao, J.; Ying, Q.; Isobe, H.; Sawamura, M.; Nakamura, E.; Chu, B. Multilayer vesicles and vesicle clusters formed by the fullerene-based surfactant C60(CH3)5K. *J. Colloid Interface Sci.* **2004**, *275*, 632−641.
(44) Guida, V. Thermodynamics and kinetics of vesicles formation processes. *Adv. Colloid Interface Sci.* **2010**, *161*, 77−88.
(45) Almgren, M.; Rangelov, S. Spontaneously Formed Non-equilibrium Vesicles of Cetyltrimethylammonium Bromide and Sodium Octyl Sulfate in Aqueous Dispersions. *Langmuir* **2004**, *20*, 6611−6618.
(46) Choi, H. S.; Kim, J. W.; Cha, Y.-N.; Kim, C. A quantitative nitroblue tetrazolium assay for determining intracellular superoxide anion production in phagocytic cells. *J. Immunoassay Immunochem.* **2006**, *27*, 31−44.
(47) Troshin, P. A.; Astakhova, A. S.; Lyubovskaya, R. N. Synthesis of fullerenols from halofullerenes. *Fullerenes, Nanotubes, Carbon Nanostruct.* **2005**, *13*, 331−343.
(48) Jovanovic, S. V.; Steenken, S.; Tosic, M.; Marjanovic, B.; Simic, M. G. Flavonoids as Antioxidants. *J. Am. Chem. Soc.* **1994**, *116*, 4846−4851.
(49) Schildknecht, S.; Pape, R.; Müller, N.; Robotta, M.; Marquardt, A.; Bürkle, A.; Drescher, M.; Leist, M. Neuroprotection by minocycline caused by direct and specific scavenging of peroxynitrite. *J. Biol. Chem.* **2011**, *286*, 4991−5002.
(50) Torchilin, V. P. Structure and design of polymeric surfactant-based drug delivery systems. *J. Controlled Release* **2001**, *73*, 137−172.
(51) Hrenovic, J.; Ivankovic, T. Toxicity of anionic and cationic surfactant to Acinetobacter junii in pure culture. *Cent. Eur. J. Biol.* **2007**, *2*, 405−414.
(52) Alkilany, A. M.; Nagaria, P. K.; Hexel, C. R.; Shaw, T. J.; Murphy, C. J.; Wyatt, M. D. Cellular Uptake and Cytotoxicity of Gold Nanorods: Molecular Origin of Cytotoxicity and Surface Effects. *Small* **2009**, *5*, 701−708.
(53) Schildknecht, S.; Pöltl, D.; Nagel, D. M.; Matt, F.; Scholz, D.; Lotharius, J.; Schmieg, N.; Salvo-Vargas, A.; Leist, M. Requirement of a dopaminergic neuronal phenotype for toxicity of low concentrations of 1-methyl-4-phenylpyridinium to human cells. *Toxicol. Appl. Pharmacol.* **2009**, *241*, 23−35.
(54) Nazari, M.; Kurdi, M.; Heerklotz, H. Classifying surfactants with respect to their effect on lipid membrane order. *Biophys. J.* **2012**, *102*, 498−506.
(55) Rabbel, H.; Werner, M.; Sommer, J.-U. Interactions of amphiphilic triblock copolymers with lipid membranes: modes of interaction and effect on permeability examined by generic Monte Carlo simulations. *Macromolecules* **2015**, *48*, 4724−4732.
(56) le Maire, M.; Champeil, P.; Møller, J. V. Interaction of membrane proteins and lipids with solubilizing detergents. *Biochim. Biophys. Acta, Biomembr.* **2000**, *1508*, 86−111.

DOI: 10.1021/acsami.8b07032
ACS Appl. Mater. Interfaces 2018, 10, 23638−23646